

Segmental analysis by speckle-tracking echocardiography of the left ventricle response to isoproterenol in male and female mice

Elisabeth Walsh-Wilkinson¹, Marie Arsenault¹, Jacques Couet^{Corresp. 1}

¹ Groupe de recherche sur les valvulopathies, Centre de recherche de l'Institut 7 universitaire de cardiologie et de pneumologie de Quebec, Universite Laval,, Quebec, Quebec, Canada

Corresponding Author: Jacques Couet
Email address: jacques.couet@med.ulaval.ca

We studied by conventional and speckle-tracking echocardiography (STE) the response of the left ventricle (LV) to a three-week continuous infusion of isoproterenol (Iso), a non-specific beta-adrenergic receptor agonist in male and female C57Bl6/J mice. Before and after Iso (30 mg/kg/day), we characterized LV morphology and function as well as global and segmental strain. We observed that Iso reduced LV ejection in both male (-8.7%) and female (-14.7%) mice. Several diastolic function parameters were also negatively regulated in males and females such as E/A, E/e', isovolumetric relaxation time. Global longitudinal (GLS) and circumferential (GCS) strains were similarly reduced by Iso in both sexes, GLS by 31% and GCS by about 20%. For the segmental LV analysis, we measured strain, strain rate, reverse strain rate, peak speckle displacement, peak speckle velocity and segmental volume changes in the parasternal long-axis. We observed that radial strain of the LV posterior segments, were more severely modulated by Iso than the anterior wall in males. In females, on the other hand, both posterior and anterior wall segments were negatively impacted by Iso. Longitudinal strain showed similar results to radial strain for both sexes. Strain rate, on the other hand, was only moderately changed by Iso. Reverse strain rate measurements, (an index of diastolic function) showed that similar LV segments to strain were negatively regulated by Iso. Biological sex differences were relatively moderate. Some STE parameters being more severely impacted in one sex compared to the others and vice-versa. Taken together, our study indicates that strain analysis can identify regions of the LV that are more negatively affected by a cardiotoxic agent such as Iso.

1 Segmental analysis by speckle-tracking 2 echocardiography of the left ventricle 3 response to isoproterenol in male and 4 female mice

5 **Élisabeth Walsh-Wilkinson¹, Marie Arsenault¹, and Jacques Couet¹**

6 ¹Groupe de recherche sur les valvulopathies, Centre de recherche de l'Institut
7 universitaire de cardiologie et de pneumologie de Québec, Université Laval, Quebec,
8 Quebec, Canada

9 Corresponding author:

10 Jacques Couet¹

11 Email address: jacques.couet@med.ulaval.ca

12 **ABSTRACT**

13 We studied by conventional and speckle-tracking echocardiography (STE) the response of the left ventricle
14 (LV) to a three-week continuous infusion of isoproterenol (Iso), a non-specific beta-adrenergic receptor
15 agonist in male and female C57Bl6/J mice. Before and after Iso (30 mg/kg/day), we characterized LV
16 morphology and function as well as global and segmental strain. We observed that Iso reduced LV
17 ejection in both male (-8.7%) and female (-14.7%) mice. Several diastolic function parameters were
18 also negatively regulated in males and females such as E/A, E/E', isovolumetric relaxation time. Global
19 longitudinal (GLS) and circumferential (GCS) strains were similarly reduced by Iso in both sexes, GLS by
20 31% and GCS by about 20%. For the segmental LV analysis, we measured strain, strain rate, reverse
21 strain rate, peak speckle displacement, peak speckle velocity and segmental volume changes in the
22 parasternal long-axis. We observed that radial strain of the LV posterior segments, were more severely
23 modulated by Iso than the anterior wall in males. In females, on the other hand, both posterior and
24 anterior wall segments were negatively impacted by Iso. Longitudinal strain showed similar results to
25 radial strain for both sexes. Strain rate, on the other hand, was only moderately changed by Iso. Reverse
26 strain rate measurements, (an index of diastolic function) showed that similar LV segments to strain were
27 negatively regulated by Iso. Biological sex differences were relatively moderate. Some STE parameters
28 being more severely impacted in one sex compared to the others and vice-versa. Taken together, our
29 study indicates that strain analysis can identify regions of the LV that are more negatively affected by a
30 cardiotoxic agent such as Iso.

31 **INTRODUCTION**

32 Women represent over lifetime 50% of heart failure (HF) patients Pfeffer et al. (2019). Clinical presentation
33 of HF is different between the sexes. HF is often more ischemic in men, happens at a younger age and
34 leads to reduced ejection fraction (EF). In women, HF happens at older age and often as a consequence
35 of hypertensive disease. Moreover, several cardiomyopathies are more prevalent in women, namely
36 Takotsubo cardiomyopathy. This stress-induced cardiomyopathy (SIC) has been modeled in rodents
37 by creating an acute and severe adrenergic overstimulation using norepinephrine or the non-selective
38 beta-adrenergic agonist, isoproterenol Sachdev et al. (2015).

39 Beta-adrenergic overstimulation using isoproterenol (Iso) has been often used to induce cardiac toxicity
40 in small rodent models Gomes et al. (2013); Chang et al. (2018); Kudej et al. (1997). Sometimes described
41 as a HF model (systolic and/or diastolic), a cardiac hypertrophy model or a SIC model (Takotsubo-like
42 syndrome) Puhl et al. (2016); Wallner et al. (2016); Sachdeva et al. (2014); Shao et al. (2013a,b); Angelini
43 and Gamero (2019), use of Iso on rats or mice has been the object of an important amount of literature.

44 Many regimens of Iso administration to rodents have been used in past studies such as a single

45 high dose bolus, several injections over days as well as continuous infusion using osmotic micro-pumps
46 implanted sub-cutaneously or intra-peritoneally, or micro-pellets at different dosages and for various
47 duration An et al. (2016); Chang et al. (2018); Ali et al. (2019); Shao et al. (2013b); Ma et al. (2011). This
48 diversity of experimental set-ups makes the comparison between studies sometimes difficult as the goals
49 pursued by the authors were often different. In addition, as for many pre-clinical studies, most experiments
50 were conducted in male animals and less often in females, especially in rats. In mice, more studies were
51 performed using females but again, few studies studied in parallel both sexes Zhu et al. (2016).

52 Sex-related differences in the Iso model have been studied using echocardiography in C57B16 mice
53 infused for 7 or 14 days (10 mg/kg/day) but relatively few differences in either systolic or diastolic cardiac
54 function were found. Most of the differences were identified at tissue level Zhu et al. (2016). More
55 recently in another study, no sex differences were found in mice treated with Iso for 14 days Grant et al.
56 (2020).

57 In the present study, we wished to document the left ventricular (LV) response to a beta-adrenergic
58 receptor-mediated insult using the Iso mouse model and to possibly identify morphological and functional
59 sex differences. We used a higher dosage of Iso (30 mg/kg/day) for a longer infusion period (21 days).
60 Using conventional and speckle tracking echocardiography (STE), we evaluated if LV dysfunction was
61 present and then performed a regional study of this dysfunction.

62 Our results indicate that Iso induced both systolic and diastolic function impairments in mice and that
63 only small sex differences were present in the extent of these. By STE, we showed that the response to Iso
64 is not homogeneously distributed throughout the LV wall as the posterior LV wall seems more sensitive to
65 Iso effects, at least in male mice.

66 METHODS

67 Mouse model

68 The present study was conducted within the Mouse Animal model of Sex Differences and Aging in heart
69 Failure (MASDAF) study, which follows longitudinally C57B16/J mice in order to investigate biological
70 sex and aging effects on the LV response to an insult. In this sub-study, we compared the LV response
71 of both males and females (purchased at 8 weeks of age) from Jackson Laboratory (Bar Harbor, ME,
72 USA). The animals were housed 3-5 mice per cage. Nesting material and a shelter was provided. After a
73 week of acclimatization, micro-osmotic pumps (cat. no.: 1004; Alzet, Cupertino, CA, USA), releasing
74 isoproterenol (Iso: 30 mg/kg/day; Sigma-Aldrich, Mississauga, Ont, Canada; n=10 mice/group) or vehicle
75 (saline; Ctrl.; n=8 mice/group), were implanted subcutaneously in the back of the neck and left for 21
76 days Roussel et al. (2018). The animals were monitored daily by experienced technicians for health and
77 behavior during the protocol. The animals were weighed weekly. No mouse displayed markers associated
78 with death or poor prognosis of quality of life, or specific signs of severe suffering or distress, which
79 would have led to early and immediate euthanasia. Among those, significant loss or gain of weight,
80 grooming and changes in behavior were monitored. The animals used in this study were not euthanized
81 at the end of this period but were let to survive for an additional 12 weeks. Euthanasia was performed
82 under isoflurane anesthesia. The thorax was then opened and cardiac exsanguination performed. The
83 heart was then excised and managed for storage. The protocol was approved by the Université Laval's
84 animal protection committee and followed the recommendations of the Canadian Council on Laboratory
85 Animal Care (2019-360, VRR-19-075).

86 Echocardiography

87 Echocardiography (Echo) studies were performed the day before Iso infusion started and 3 weeks later.
88 Echo images were acquired on a Vevo 3100 imaging system (VisualSonics, FujiFilm, Toronto, Canada)
89 by the same investigator and analysed off-line using Vevo LAB software. The investigator was blinded for
90 animal identification but it was not possible to do so for its sex. Animals were anesthetized and positioned
91 on a heated platform ventral side up. The concentration of isoflurane was maintained around 1.5–2.5%,
92 so the heart rate was kept between 400 and 550 beats/minute.

93 2D echo: M-mode images were recorded to measure diastolic and systolic LV wall thickness from the
94 parasternal long-axis (PSLAX) view and the short-axis (SAX) view at the papillary muscle level. From
95 these measurements, LV Mass was calculated by the VevoLab echo analysis software (VisualSonics)
96 using the following equation: $1.053 \times [(EDD+PW+IVSW)^3 - EDD^3] \times 0.8$ where: EDD is the internal
97 dimension of the LV at the end of diastole, PW is the thickness of the posterior wall at the end of diastole

98 and IVSW is the thickness of the inter-ventricular septum at the end of diastole. Fractional shortening
99 from M-mode images was calculated using the following equation: $(EDD - ESD) / EDD$ where: ESD
100 is the internal dimension of the LV at the end of systole. Pulsed wave Doppler was used to measure the
101 mitral flow from an apical four-chamber view. Early diastolic peak filling velocity (E wave), peak filling
102 velocity at atrial contraction (A wave), E wave deceleration time and the E/A ratio were obtained. The
103 early-diastolic peak velocity (E'), the late-diastolic peak velocity (A') of mitral valve annulus and E'/A'
104 as well as E/E' were obtained using tissue Doppler. LV volumes, ejection fraction (EF), stroke volume and
105 cardiac output were calculated using the Simpson's rule method from LV chamber area tracings.

106 Speckle-tracking echo: 2D echo B-mode loops were acquired from the LV PSLAX and analysed
107 using Vevo Strain software (VisualSonics). Images were acquired at 232 frames/s and strain analysis
108 was performed in the radial and longitudinal axes. Three cardiac cycles of the highest quality loops were
109 selected to avoid respiration movements, echo gel artefacts, and obstruction from the ribs. Endocardial
110 and epicardial borders were traced at mid-diastole. LV tracing was started from the anterior wall close
111 from the aorta root to the posterior wall close from the mitral valve. Vevo Strain software then built the
112 dynamic LV tracing for all selected frames. Loops were replayed to confirm validity of border tracking
113 over cardiac cycles and adjustments were made, if needed. LV myocardium was then divided into 6 equal
114 anatomical segments and peak systolic strain calculated for every segment. Strain = $(Ls - Ld) / (Ld)$ where:
115 Ls = Length at end-systole and Ld = Length at end-diastole. From this, the strain rate (SR) was calculated
116 taking into account cardiac cycle duration. Also calculated by the Vevo Strain software, were the reverse
117 strain rate (a diastolic function index), speckle displacement (mm), velocity (mm/s) as well as segmental
118 volume changes (mm^3). Segmental volume (V) changes were then calculated for each LV segment using
119 maximal Vsystolic - minimal Vdiastolic / maximal Vsystolic (over 3 cardiac cycles) and is expressed in
120 %.

121 **Statistical analysis**

122 All data are expressed as mean \pm standard error of the mean (SEM). Normality was assessed using the
123 Shapiro-Wilk test. Inter-group comparisons were conducted using Student's T-test using GraphPad Prism
124 8.4, GraphPad Software Inc., La Jolla, CA, USA). Data from Tables 1 to 3 were analysed using 2-way
125 ANOVA and Holm-Sidak post-test. $P < 0.05$ was considered statistically significant. Raw data are provided
126 in the supplemental data section.

127 **RESULTS**

128 **Isoproterenol induces systolic and diastolic impairments in male and female mice**

129 Before implantation of the micro-osmotic pump, a complete echocardiography (echo) exam was performed
130 for each animal. Baseline values are listed in Table S1 (Supplemental data). With the exception of those
131 related to the relative size of male and female animals, systolic and diastolic functions baseline parameters
132 were mostly similar between the sexes.

133 Ten of these eighteen mice of each sex were then treated for three weeks with a continuous infusion of
134 isoproterenol (Iso), a non-specific beta-adrenergic receptor agonist. On day twenty-one, osmotic pumps
135 were removed and the day after, a second echo exam was performed. As depicted in Table 1, Iso treatment
136 had relatively similar effects in male and female mice on M-mode echo measurements. End-systolic LV
137 diameter (ESD) was increased in mice of both sexes resulting in a corresponding decrease in fractional
138 shortening (-7.4% for males and -7.9% for females). As mentioned above, LV volumes were calculated
139 using the Simpson's rule method from PSLAX LV chamber area tracings. From these LV volumes,
140 ejection fraction (EF) was then calculated. Both end-diastolic (EDV) and end-systolic volumes (ESV)
141 were increased after Iso treatment, respectively by 23% and 49% in males and by 14% (not significant; ns)
142 and 60% in females. This resulted in lowered ejection fraction for both male (-8.7%) and female (-14.7%)
143 mice compared to control animals (Ctrl). Stroke volume was maintained in males and tended to decrease
144 in females (ns). Cardiac output was lower in Iso-treated mice.

145 Diastolic parameters were also modified by Iso. E wave measured by pulse-wave Doppler, was
146 decreased in male mice but not in females as described in Table 2. We then measured E' and A' waves
147 of the mitral valve annulus by tissue Doppler. E' wave was significantly reduced by 34% in males. E/E'
148 ratio, an index of diastolic function was significantly increased by Iso in males (30%). Only a tendency
149 was registered for females (+20%). Isovolumetric relaxation time (IVRT) was significantly longer in both
150 Iso groups compared to controls (+40% in males and +20% in females, respectively).

Table 1. Left ventricle morphology and systolic function in male and female mice receiving or not isoproterenol for 3 weeks. Ctrl: control, Iso: isoproterenol treatment, BW: body weight, LV: left ventricle mass, EDD: end-diastolic LV diameter, ESD: end-systolic diameter, IVS: inter-ventricular septum, PW: posterior wall, RWT: relative wall thickness, FS: fractional shortening, EDV: end-diastolic volume, ESV: end-systolic volume, SV: stroke volume, EF: ejection fraction, HR: heart rate, bpm: beats per minute and CO: cardiac output. Values are expressed as the mean \pm SEM. Two-way ANOVA statistical analysis results are displayed for each factor, sex and iso, respectively. Inter-group p values were calculated using Holm-Sidak post-test. a: $p < 0.05$, b: $p < 0.01$ and c: $p < 0.001$ between Ctrl and Iso groups, respectively. ns: not significant.

Parameters	M Ctrl (n=8)	M Iso (n=10)	F Ctrl (n=8)	F Iso (n=10)	Sex	Iso
BW, g	25.0 \pm 0.31	27.9 \pm 0.53b	19.9 \pm 0.28	20.8 \pm 0.45	<0.0001	ns
Tibia, mm	21.0 \pm 0.08	21.7 \pm 0.10d	20.5 \pm 0.08	20.3 \pm 0.13	<0.001	ns
M-mode						
EDD, mm	3.8 \pm 0.03	3.9 \pm 0.07	3.6 \pm 0.06	3.6 \pm 0.07	<0.001	ns
ESD, mm	2.6 \pm 0.08	2.9 \pm 0.11a	2.3 \pm 0.05	2.6 \pm 0.07b	<0.01	<0.001
IVS, mm	0.82 \pm 0.02	0.82 \pm 0.02	0.76 \pm 0.01	0.77 \pm 0.02	<0.001	ns
PW, mm	0.84 \pm 0.01	0.83 \pm 0.02	0.78 \pm 0.01	0.75 \pm 0.02	<0.0001	ns
RWT	0.44 \pm 0.01	0.42 \pm 0.01	0.43 \pm 0.01	0.42 \pm 0.01	ns	ns
FS, %	32.2 \pm 1.69	24.8 \pm 1.52b	35.4 \pm 0.98	27.5 \pm 0.86c	<0.05	<0.0001
LV, mg	86 \pm 2.1	95 \pm 4.1	76 \pm 2.6	75 \pm 2.7	<0.0001	ns
iLV, mg/g	3.4 \pm 0.10	3.4 \pm 0.11	3.8 \pm 0.14	3.6 \pm 0.11	<0.01	ns
Simpson						
EDV, μ l	54.6 \pm 1.83	66.9 \pm 3.62b	44.6 \pm 0.74	51.0 \pm 2.45	<0.0001	<0.01
ESV, μ l	23.4 \pm 0.72	34.8 \pm 2.78b	17.1 \pm 0.34	27.4 \pm 2.13b	<0.01	<0.0001
SV, μ l	31.2 \pm 1.39	32.1 \pm 1.91	27.5 \pm 0.56	23.6 \pm 1.19	<0.001	ns
EF, %	57.1 \pm 1.01	48.4 \pm 2.19a	61.7 \pm 0.55	47.0 \pm 2.80c	ns	<0.0001
HR, bpm	494 \pm 17.9	415 \pm 10.0b	441 \pm 16.8	448 \pm 9.0	ns	<0.05
CO, ml/min	15.3 \pm 0.69	13.3 \pm 0.73	12.2 \pm 0.56	10.6 \pm 0.60	<0.0001	<0.01

Table 2. Left ventricle diastolic parameters in male and female mice receiving or not isoproterenol for 3 weeks. IVRT: isovolumetric relaxation time. Values are expressed as the mean \pm SEM. Two-way ANOVA statistical analysis results are displayed for each factor, sex and iso, respectively. Inter-group p values were calculated using Holm-Sidak post-test. a: $p < 0.05$, b: $p < 0.01$, c: $p < 0.001$ and d: $p < 0.0001$ between Ctrl and Iso groups, respectively. ns: not significant.

Parameters	M Ctrl (n=8)	M Iso (n=10)	F Ctrl (n=8)	F Iso (n=10)	Sex	Iso
E, mm/s	662 \pm 23.6	551 \pm 18.4c	578 \pm 15.6	579 \pm 14.2	ns	<0.01
A, mm/s	430 \pm 21.7	380 \pm 9.0	363 \pm 10.1	375 \pm 16.9	<0.05	ns
E/A	1.55 \pm 0.03	1.45 \pm 0.03	1.60 \pm 0.05	1.57 \pm 0.07	ns	ns
E dec.time, ms	20.0 \pm 1.20	25.2 \pm 1.65	18.8 \pm 0.70	22.4 \pm 1.88	ns	<0.01
E', mm/s	27.6 \pm 1.49	18.3 \pm 1.04d	26.1 \pm 1.61	22.3 \pm 0.81	ns	<0.0001
E/E'	24.2 \pm 1.45	31.4 \pm 1.57a	22.3 \pm 1.42	30.5 \pm 2.54	<0.05	<0.001
A', mm/s	19.3 \pm 0.44	13.8 \pm 0.98c	20.4 \pm 1.41	16.4 \pm 0.49a	ns	<0.0001
E'/A'	1.43 \pm 0.06	1.36 \pm 0.04	1.29 \pm 0.04	1.43 \pm 0.06	ns	ns
IVRT, ms	15.1 \pm 0.32	21.1 \pm 0.57d	16.1 \pm 0.61	19.4 \pm 0.93b	ns	<0.0001

151 In Table 3 is illustrated the evolution of global longitudinal (GLS) and global circumferential (GCS)
 152 strains in male and female mice receiving Iso. Global strain measurements take into consideration the
 153 entire LV wall comparing the LV inner contour length changes. GLS is calculated from PSLAX view
 154 and GCS from SAX view. For both parameters, GLS and GCS, more negative values are associated with
 155 better fractional change of the myocardium during the cardiac cycle. In control animals, GLS and GCS
 156 values were similar between the sexes. After 3 weeks of Iso infusion, GLS values became significantly

157 less negative in both males (+31%) and females (+31%). As for GCS, it worsened following Iso similarly
158 in males (+17%) and in females (+23%).

Table 3. Global LV strain parameters in male and female mice treated or not with isoproterenol for 3 weeks. GLS: global longitudinal strain and GCS: global circumferential strain. Values are expressed as the mean \pm SEM. Two-way ANOVA statistical analysis results are displayed for each factor, sex and iso, respectively. Inter-group p values were calculated using Holm-Sidak post-test. c: $p < 0.001$ and d: $p < 0.0001$ between Ctrl and Iso groups, respectively. ns: not significant.

	M Ctrl (n=8)	M Iso (n=10)	F Ctrl (n=8)	F Iso (n=10)	Sex	Iso
GLS, %	-19.1 \pm 0.6	-13.1 \pm 0.8d	-20.3 \pm 0.8	-14.0 \pm 0.9c	ns	<0.0001
GCS, %	-29.4 \pm 0.9	-24.3 \pm 1.1c	-32.8 \pm 1.1	-25.2 \pm 0.7d	ns	<0.0001

159 Segmental analysis using speckle tracking echocardiography (STE) points toward a non- 160 uniform LV response to Iso in males

161 The LV was divided into six segments for the PSLAX view, as described in Figure 1A. This allowed us to
162 investigate if the effects of Iso infusion were globally distributed along the LV endocardial wall or if one
163 or many segments were more seriously affected than others.

164 Using segmental analysis, we compared strain (Figure 1) at baseline (Pre-Iso) and after Iso in male
165 and female mice. As illustrated in Figure 2 B-E, radial and longitudinal strains were reduced by Iso in
166 males for all three posterior LV wall segments, whereas anterior ones were left mostly unchanged. Radial
167 strain of two posterior wall segments (base and mid) was reduced in females. In addition, radial strain
168 for all LV anterior wall segments was reduced. Average radial and longitudinal strains (all segments; in
169 black) were negatively modulated by Iso for both male and female mice.

170 We grouped data from the segmental strain analysis either as from the base, the mid-ventricle or the
171 apex regardless of the posterior or the anterior walls. We did the same for the anterior or the posterior wall
172 data that were analysed together regardless if they originated from the base, mid-ventricle or apex Kudej
173 et al. (1997). As illustrated in Figure 2 E-L, both radial and longitudinal strains were reduced for the base
174 LV segment in male and female mice. Mid LV section radial strain was reduced for both sexes. This was
175 also the case for the longitudinal strain in males as well as the apex longitudinal strain in male and female
176 animals. We then compared if the posterior wall strain was more affected by iso than the anterior wall. In
177 females, both radial and longitudinal strains were reduced by iso relatively to the same extent (-30%). In
178 males, the radial strain was significantly decreased for the posterior wall but not for the anterior one. The
179 longitudinal strain was reduced for both walls but this decrease was more important for the posterior wall
180 than the anterior one (-39% vs. -18%, respectively).

181 As illustrated in Video S1 (males) and Video S2 (females) (Supplemental data), LV wall deformation
182 after Iso was markedly reduced and sometimes showed features of an infarct in the posterior wall near the
183 apex. When LV movement tendency was expressed using velocity vectors as illustrated in Figure 2, it
184 can be appreciated that both in systole and diastole, the reduction of the length and the changes in the
185 orientation of velocity vectors induced by Iso.

186 Peak strain rate (SR) represents a systolic function index since it indicates the maximal rate of
187 deformation (strain) during systole. Reverse peak SR happens during the passive LV filling phase of
188 diastole (Figure 3A) and had been proposed as a new index of diastolic function Schnelle et al. (2018).

189 Changes in radial and longitudinal strain rates (SR) caused by Iso were relatively minor and concen-
190 trated on the posterior segments in males and females (Figure 4 B-E). Peak reverse SR showed a pattern
191 reminiscent of those of strain and SR where LV posterior segments were negatively modified by Iso in
192 both males and females (Figure 4 F-H). Several anterior wall segments were also affected but mostly in
193 females.

194 Peak speckle displacement and peak speckle velocity are analogous to strain and strain rate although
195 they are not expressed relative to a second point in the myocardium as for strain and SR. Original speckle
196 position or speckle velocity is determined from the R-wave and is arbitrarily fixed to 0. Radial speckle
197 displacement and velocity were reduced, mainly for the posterior wall segments in males and females.
198 Displacement was also reduced for the anterior wall in females. In the longitudinal direction, peak speckle

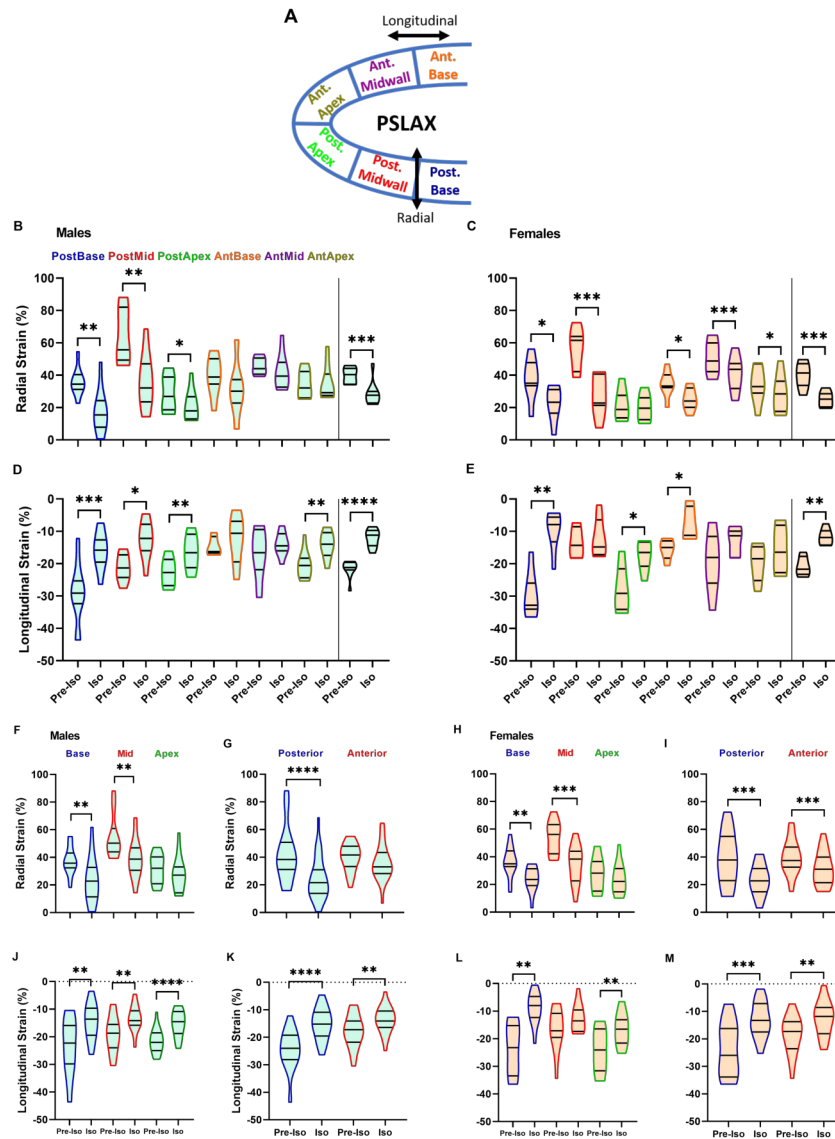


Figure 1. Speckle tracking strain analysis. A. Radial and longitudinal strains can be obtained using the parasternal long axis (PSLAX) view. The six segments are also identified. Characters colors corresponds to those used in the graphs for each of these LV segments. Ant: anterior, Post: posterior. Radial (B-C) and longitudinal (D-E) peak strains were obtained using the parasternal long axis view. The six segments are identified. Characters colors corresponds to those used in the graphs for each of these LV segments. Radial (F-G and H-I) and longitudinal (J-K and L-M) peak strains were grouped either as from the base, the mid-section or the apex or as from the anterior or the posterior segments in males (left panels) and females (right panels). Ant: anterior, Post: posterior. Males are represented on the left panels and females on the right. Results are represented as violin plots (n=8-10). Inner black lines represent quartiles of the data. Significance between groups was calculated with paired Student's T-test. *: $p < 0.05$, **: $p < 0.01$, ***: $p < 0.001$ and ****: $p < 0.0001$ between corresponding pre-Iso and Iso animals.

199 displacement remained stable in males and was reduced for only one segment (anterior base) in females.
 200 A similar situation was observed for longitudinal velocity of the LV wall (Figure S1; supplemental data).

201 From the endocardial and epicardial combined LV tracings, the Vevo Strain software can produce
 202 an estimate of the volume of each LV segment. We determined for each segment both the minimal
 203 (diastole) and maximal (systole) volumes and calculated the segmental volume change (in %) as described

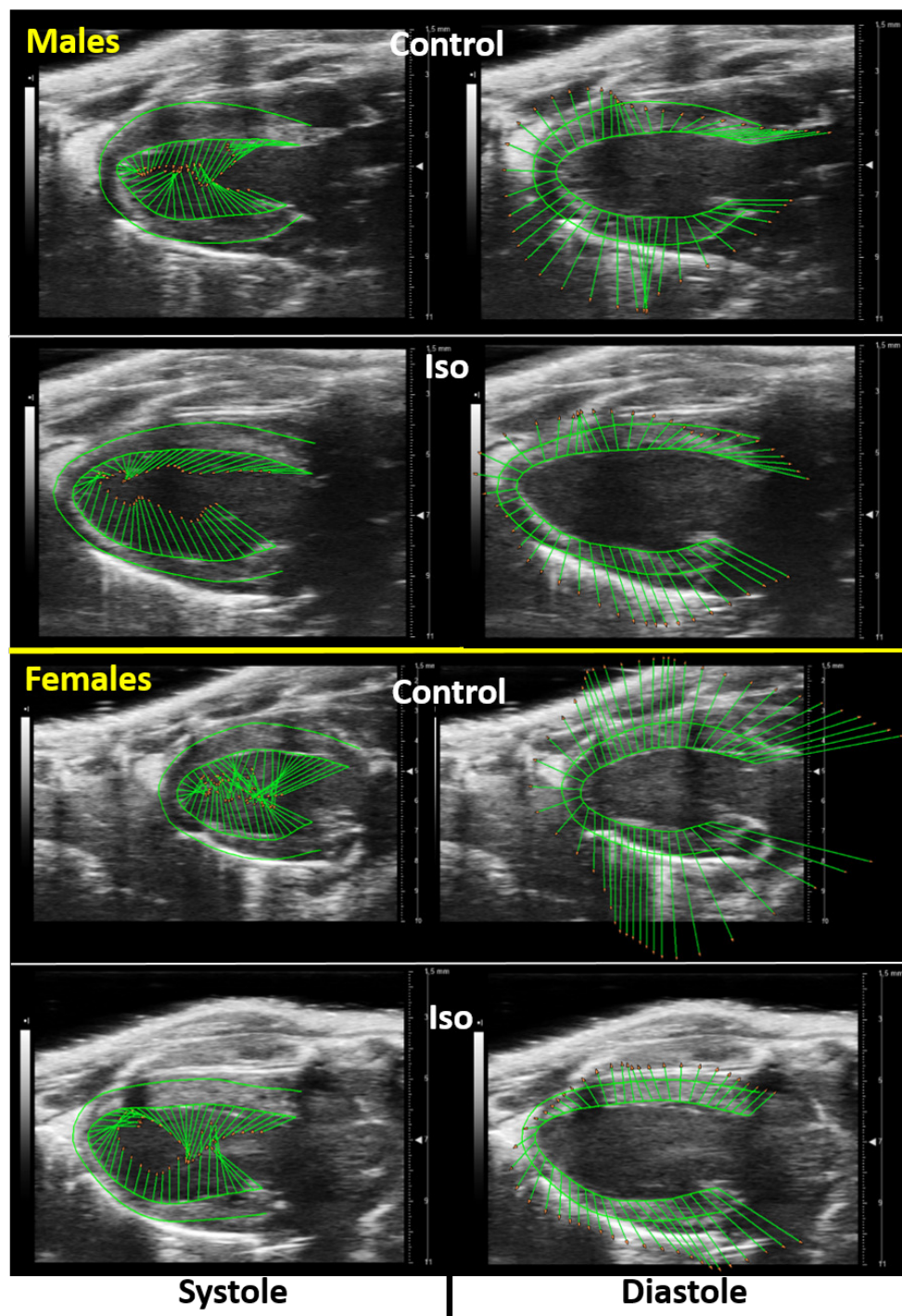


Figure 2. PSLAX LV wall trace tendency before and after Iso. LV wall trace tendency are expressed as velocity vectors for >48 points around the endocardium in systole (left panels) and diastole (right panels) before and after Iso in males (top panels) and females mice (bottom panels). Images of velocity vectors corresponds to the maximal peak (systole) and minimal peak (diastole) of the average curve of all six segments curves for speckle velocity in PSLAX. As evidenced by these PSLAX B-mode views, velocity vectors orientation and length varies during the cardiac cycle. Vertical (radial) and horizontal (longitudinal) components of each vector do not correspond necessarily to the respective peak value of each orthogonal component.

204 in the Methods section. Results are illustrated in Figure 4. Posterior segments had a general decrease of
205 segmental volume change during the cardiac cycle for both male and female mice. Anterior segments
206 were also reduced in females.

207 DISCUSSION

208 In the present study, we demonstrated that the LV response to beta-adrenergic sur-activation using Iso,
209 resulted in both systolic and diastolic function impairments in mice of both sexes. Loss of ejection fraction
210 relative to baseline was more important in females although it resulted in levels similar for both sexes
211 post-Iso. More diastolic function parameters were negatively altered in males compared to females. Using
212 speckle-tracking echocardiography, we proceeded to a thorough investigation of strain, strain rate and
213 other related parameters. In males, we observed that the LV posterior wall was in general more negatively
214 affected by Iso than the anterior wall. This was true for strain in both radial and longitudinal directions. In
215 females, strain in the LV posterior wall was also negatively reduced but the anterior wall was also affected
216 making the effects of Iso more global.

217 Most baseline values for the different parameters obtained from STE (strain, SR, and rSR) were
218 similar between males and females. Radial peak speckle displacement and velocity for certain segments
219 were significantly smaller in females, which is related to their smaller heart size. To our knowledge, this
220 study is the first to report segmental LV wall displacement and velocity data from normal young adult
221 mice.

222 Conventional echocardiography

223 Systolic function as estimated by ejection fraction (EF) was relatively more reduced in females than in
224 males. Baseline EF values were higher in females. Various methods are available for the evaluation of EF
225 by echo. The availability for small animals of four-dimensional (4D) echo LV chamber reconstruction
226 over the cardiac cycle adds another way to estimate EF. In this study, we finally opted for the Simpson's
227 method from LV chamber area tracings in PSLAX instead of 4D echo. Four-dimensional echo, in our
228 hands, probably underestimated LV volume, which lead to incorrect calculations of LV volumes, stroke
229 volume, ejection fraction and so forth. Depending on the method, EF estimates went from being in the
230 65-70% range using M-mode, 57-62% range using Simpson's method to 55-60% (PSLAX) and 45-50%
231 (SAX) using 4D echo in normal mice. In addition, Iso effects seemed to be masked using 4D echo and
232 variability was higher using this method. See Table S2 in supplemental data section for comparison of the
233 various methods of evaluating EF.

234 Several factors can limit acquisition of quality 4D echo scans in rodents as described before by several
235 studies Grune et al. (2018); Damen et al. (2017); Rutledge et al. (2020); Grant et al. (2020). One is
236 interference from anatomical structures (sternum, ribs and lungs) that often obscure parts of the heart,
237 making it difficult to visualize and to trace LV walls. Working with those low-quality 4D echo scans can
238 significantly increase intra-observer variability and thus, reduce reproducibility. Therefore, we decided to
239 rely on the Simpson method for volume measurements.

240 Isoproterenol treatment resulted into a lowering of EF to similar levels in males and females, around
241 47-48%. It is from the differences in baseline EF between males and females that originated the more
242 important loss in females. Since baseline EF was not significantly different between the sexes using the
243 other methods (M-mode or 4D-echo), we have to remain cautious with the affirmation that Iso treatment
244 had a more negative effect on EF in females. Nevertheless, it is interesting that LV dilatation (EDV
245 variation) was more important after Iso in males, whereas ESV increased more in females suggesting
246 somewhat different paths to systolic function impairments.

247 Despite these discrepancies between the methods used to evaluate EF, it was clear that Iso increased
248 both systolic LV diameters and volumes in mice. A LV dilation was also apparent in 2D B-mode views,
249 whereas wall thickness seemed to remain remained stable (see Figure 2, Videos S1 and S2). This LV
250 remodeling helped preserve cardiac output although a trend for a decrease was present. It is difficult
251 to affirm that mice were experiencing symptoms of HF after Iso, especially since cardiac output was
252 mostly preserved. HF in small rodents is often recognized by increased lungs weight after euthanasia or
253 decreased exercise performance Gomes et al. (2013). We did not test in our animals resistance to forced
254 exercise.

255 In the case of diastolic parameters measured either by pulse-wave Doppler or tissue Doppler, many of
256 them were negatively modulated by Iso in male mice. In females, only those measured by tissue Doppler

257 were affected by Iso and, to a lesser extent than for males. As in humans, defining diastolic dysfunction by
258 echo is difficult although it is clear that Iso treatment caused diastolic function impairments, especially in
259 male mice. Since, the hearts of the animals were not studied *in vitro* afterwards, it is difficult to speculate
260 further for the reason of these observations.

261 Myocardial interstitial fibrosis is often related to diastolic dysfunction. Iso treatment has been shown
262 to induce fibrosis in mice in many other studies. Collagen production was shown to be more important
263 in male mice receiving Iso than in females Zhu et al. (2016). Among the other mechanisms that have
264 been proposed to explain HF induced by Iso is an increased rate of cardiomyocyte apoptosis Zhuo et al.
265 (2013). Sur-activation of the beta-adrenergic system by Iso also imposes an increased cardiac workload,
266 which is associated with increased consumption of oxygen by the myocardium. This can lead to increased
267 production of reactive oxygen species Ma et al. (2015). An additional mechanism that could explain
268 negative effects of Iso is lipotoxicity. In an acute model of Iso-induced stress cardiomyopathy, rapid lipid
269 accumulation was noticed as soon as two hours after injection. It is not clear if here, in this chronic model,
270 this intracellular lipid accumulation is present or lasts for days but this does exclude a possible toxicity
271 for the cardiac myocytes leading to apoptosis Shao et al. (2013b).

272 **Speckle-tracking echocardiography**

273 In this study, conventional echo was able to highlight LV anomalies both morphological and functional.
274 Our study design did not aim at testing if strain analysis would be more sensitive for early detection
275 of dysfunction as it was done in previous studies An et al. (2016); Li et al. (2014); Peng et al. (2009);
276 Szymczyk et al. (2013). Our goal was to evaluate if additional and valuable information could be obtained
277 using STE such as strain and SR but also reverse SR, speckle displacement, speckle velocity and segmental
278 volume changes.

279 Using the strain analysis, we observed that the LV posterior wall was in general more negatively
280 modulated by Iso than the anterior wall. The base and the mid-ventricle segments were the most affected
281 and the apex, to a lesser extent. This trend was clearer in males although posterior segments were
282 also impacted in females. Obviously, our Iso treatment being longer and more severe has triggered a
283 compensatory response An et al. (2016). LV dilatation had time to take place mostly in males which
284 has to be accompanied by a concomitant extracellular matrix remodeling. Fibrosis was probably present
285 as described in other studies looking at Iso effects on the mouse myocardium Zhuo et al. (2013); Grant
286 et al. (2020). In addition, this long exposure to Iso most likely brought a general down-regulation of
287 beta-adrenergic receptors leaving non receptor-mediated Iso effects to play a significant part in our
288 observations. The reason for the posterior wall being more sensitive to Iso than the anterior wall still is
289 not clear. Differences in LV regional beta-receptor subtypes density have been reported before. Greater
290 apical beta-adrenergic receptor density or responsiveness has been described in humans, dogs, rats, cats
291 and rabbit hearts Mori et al. (1993); Kawano et al. (2003); Heather et al. (2009); Lathers et al. (1986);
292 Mantravadi et al. (2007). Use of Iso infusion in order to create infarct-like damages and HF as well as
293 for inducing Takotsubo-like syndrome selectively targets the LV apex Paur et al. (2012); Rona (1959);
294 Shao et al. (2013c,b). This basal-apex gradient of beta-adrenergic receptors responsiveness has thus been
295 well-described. Here, our observation made in the PSLAX now includes an additional axis for a possible
296 antero-posterior gradient in beta-adrenergic receptors sensitivity to suractivation. Here, we could only
297 describe this observation without providing satisfactory explanations for the reasons for this. The complex
298 3D architecture of the myocardium may provide clues but more studies are thus needed to provide new
299 insights about this intriguing observation.

300 Speckle peak displacement data at baseline show that in the radial direction, posterior segments are
301 more mobile than anterior ones (Figure S1). This is associated with larger radial wall velocities for these
302 posterior LV segments. Here too, it was these posterior segments that were more negatively targeted by Iso
303 for both peak displacement and peak velocity. In the longitudinal direction, baseline values were relatively
304 similar for posterior and anterior segments. Effects of Iso were also less important in the longitudinal
305 direction. Radial displacement and velocity in males were clearly more reduced for the posterior wall. In
306 females, both the posterior and anterior walls were both negatively modulated by Iso.

307 As illustrated in Figure 2, velocity vectors originating from the LV base (and the apex) show a more
308 important longitudinal component than the radial one. For the mid-ventricle segments, it is the opposite
309 and the radial component of the velocity vectors is more important. Strain and SR measurements are
310 expressed relative to a baseline position at the initiation of systole (EKG R-wave). They do not provide

311 however, a clear evaluation of the changes in the direction (more radial or more longitudinal) of these
312 vectors after Iso treatment. These vectors also provide information about LV relaxation. This illustrates
313 the high complexity of cardiac contraction and relaxation and the difficulty to assess regional LV dynamic
314 response using only one dimension at a time, here radial vs. longitudinal.

315 Reverse strain rate has been proposed as an index of diastolic function in mice Schnelle et al. (2018).
316 Considering that most parameters measured by STE are systolic in nature, reverse strain rate can constitute
317 an interesting window to the kinetics of LV relaxation, at least during the passive filling. It is interesting
318 to notice that again, the posterior wall segments in males are the ones with the more reduced reverse SR
319 suggesting LV stiffening caused by Iso seems to target mainly this region.

320 Segmental volume changes confirmed that the posterior wall was more targeted by Iso in males than
321 its counterpart. In females, the action of Iso was again more global. In the mid-ventricle SAX view, all 6
322 segments in males had diminished volume changes during the cardiac cycle. This parameter is interesting
323 for its relatively low intra-group variability, which can provide a better sensitivity to the early myocardial
324 response to an insult. Again, our study design did not allow us to test this but this should be investigated
325 in further studies.

326 STE strain analysis has been performed in the past in Iso-treated mice. In male mice receiving Iso
327 for either 3 or 7 days, global radial and longitudinal strain and strain rate were reduced in PSLAX and
328 only strain rates were reduced in SAX. When concentrating on LV wall segments in PSLAX, the authors
329 found no regional differences suggesting that Iso effects on the LV after 3 or 7 days were mostly global
330 An et al. (2016). Their dosage of Iso used was lower (5 vs. 30 mg/kg here) and the duration shorter
331 making it difficult to make comparison with our work. It is probable that in the present study, more
332 chronic mechanisms took place at the cellular and molecular levels, as mentioned above. Interestingly,
333 after only 3 days, An and collaborators observed increased myocardial fibrosis and hypertrophy. They did
334 not mention if chamber dilatation was present but reported LV wall thickening, which was not the case
335 in our mice after three weeks of Iso An et al. (2016).

336 We thus observe a clear reduction of global strain measurements in our animals and they were similar
337 between males and females. These parameters are highly sensitive to detect cardiac dysfunction but do
338 not provide regional information. Since most sex differences we observed were present at the regional
339 level, global longitudinal and circumferential strains were not informative.

340 **A Takotsubo cardiomyopathy model?**

341 As mentioned above, isoproterenol has been used to develop animal models of Takotsubo-like syndrome.
342 Takotsubo syndrome is defined as a "transient LV dysfunction (hypokinesia, akinesia, or dyskinesia)
343 presenting as apical, midventricular, basal, or focal ballooning" Napp and Bauersachs (2020). Adrenergic
344 over-stimulation is believed to be an important cause of this cardiomyopathy, which is more frequent
345 in post-menopausal women suggesting possible protective roles for estrogens and/or for the male sex
346 Sachdev et al. (2015).

347 The rat is usually the preferred animal model to study SIC in animals. It has been studied acutely
348 after a bolus administration of Iso or after a few days of treatment. These short regimens usually allow
349 complete recuperation of systolic function in days or weeks following Iso Shao et al. (2013a); Redfors
350 et al. (2014); Willis et al. (2015); Wallner et al. (2016); Ma et al. (2011). Beta2-adrenergic receptors
351 sarcolemmal localization was proposed for being responsible for the typical apical ballooning associated
352 with Takotsubo cardiomyopathy Wright et al. (2018). Since mid-ventricular and basal forms of this SIC,
353 other mechanisms are involved.

354 One study has been reported in mice using Iso (one single dose of 400 mg/kg) to induce a Takotsubo-
355 like syndrome Shao et al. (2013b). It did not result in global reduction of systolic function when assessed
356 2 hours after Iso injection. Segmental fractional wall thickening was measured in SAX view in these mice.
357 Interestingly, two segments had their radial strain severely reduced namely the posterior wall and inferior
358 free wall segments. These segments in SAX are part of the posterior wall in PSLAX. The four other LV
359 segments had an increased strain to compensate in their study Shao et al. (2013b). We did not observe this
360 type of compensation in our mice.

361 Most attempts to reproduce Takotsubo-like syndrome in rodents so far have relied on acute admin-
362 istration of Iso or catecholamines, suggesting that a acute surge of circulating catecholamines levels or
363 adrenergic over-stimulation are important parts of SIC etiology in patients. Known triggering factors
364 in humans such as the death of a loved one, divorce, financial loss, diagnosis of a serious disease, etc...,

365 are often related to chronic stress. In fact, circulating levels of catecholamines are seldom elevated
366 in SIC patients Pelliccia et al. (2017). This makes our study possibly relevant to mimic human SIC
367 since our mice were chronically exposed to a beta-receptor agonist. One limitation is that Iso does not
368 stimulate alpha-receptors as catecholamines do, eliminating the vasospasm component of Takotsumo
369 cardiomyopathy Pelliccia et al. (2017).

370 **Study limitations.**

371 Among the limitations of this study, tissue data could not be obtained. The animals were not euthanized at
372 the end of the present study as their longitudinal follow-up was continued for several months. Any tissue
373 data in this context would have been from LVs having a long period of recuperation after Iso treatment. It
374 will be interesting to evaluate how sex hormones and age can influence LV response to chronic Iso in the
375 future. In addition, the study in short-axis (SAX) at the level of the apex, the mid-section and the base the
376 strain and related parameters could be informative in order to correlate changes observed here in PSLAX.

377 **CONCLUSION**

378 Segmental strain analysis in mice can provide information about the regional influence of a toxic cardiac
379 insult such as the continuous infusion with for 21 days. We observed both similarities and sex-related
380 differences in our male and female mice. Both systolic and diastolic functions were negatively modulated
381 by Iso in our animals. Ejection fraction, an index of systolic function was relatively more reduced in
382 females. More diastolic function parameters were negatively changed in males. Differences between
383 sexes were relatively subtle when studied by conventional echo. By STE, we observed Iso had a more
384 global effect on the female LV whereas in males, the posterior wall was more specifically targeted.

385 **ACKNOWLEDGMENTS**

386 The authors want to acknowledge the technical help of Ms. Marine Clisson and Mr. Thomas Couët.

387 **REFERENCES**

- 388 Ali, A., Redfors, B., Lundgren, J., Alkhoury, J., Oras, J., Gan, L. M., and Omerovic, E. (2019). Effects of
389 pretreatment with cardiostimulants and beta-blockers on isoprenaline-induced takotsubo-like cardiac
390 dysfunction in rats. *Int J Cardiol*, 281:99–104.
- 391 An, X., Wang, J., Li, H., Lu, Z., Bai, Y., Xiao, H., Zhang, Y., and Song, Y. (2016). Speckle tracking
392 based strain analysis is sensitive for early detection of pathological cardiac hypertrophy. *PLoS One*,
393 11(2):e0149155.
- 394 Angelini, P. and Gamero, M. T. (2019). What can we learn from animal models of takotsubo syndrome?
395 *Int J Cardiol*, 281:105–106.
- 396 Chang, S. C., Ren, S., Rau, C. D., and Wang, J. J. (2018). Isoproterenol-induced heart failure mouse
397 model using osmotic pump implantation. *Methods Mol Biol*, 1816:207–220.
- 398 Damen, F. W., Berman, A. G., Soepriatna, A. H., Ellis, J. M., Buttars, S. D., Aasa, K. L., and Goergen,
399 C. J. (2017). High-frequency 4-dimensional ultrasound (4dus): a reliable method for assessing murine
400 cardiac function. *Tomography*, 3(4):180.
- 401 Gomes, A. C., Falcão-Pires, I., Pires, A. L., Brás-Silva, C., and Leite-Moreira, A. F. (2013). Rodent
402 models of heart failure: an updated review. *Heart Fail Rev*, 18(2):219–49.
- 403 Grant, M. K. O., Abdelgawad, I. Y., Lewis, C. A., Seelig, D., and Zordoky, B. N. (2020). Isoproterenol-
404 induced cardiac dysfunction in male and female c57bl/6 mice. *bioRxiv*.
- 405 Grune, J., Blumrich, A., Brix, S., Jeuthe, S., Drescher, C., Grune, T., Foryst-Ludwig, A., Messrogli, D.,
406 Kuebler, W. M., Ott, C., et al. (2018). Evaluation of a commercial multi-dimensional echocardiography
407 technique for ventricular volumetry in small animals. *Cardiovascular ultrasound*, 16(1):10.
- 408 Heather, L., Catchpole, A., Stuckey, D., Cole, M., Carr, C., and Clarke, K. (2009). Isoproterenol induces
409 in vivo functional and metabolic abnormalities; similar to those found in the infarcted rat heart. *Acta*
410 *physiologica Polonica*, 12(3):31.
- 411 Kawano, H., Okada, R., and Yano, K. (2003). Histological study on the distribution of autonomic nerves
412 in the human heart. *Heart and vessels*, 18(1):32–39.

- 413 Kudej, R. K., Iwase, M., Uechi, M., Vatner, D. E., Oka, N., Ishikawa, Y., Shannon, R. P., Bishop, S. P.,
414 and Vatner, S. F. (1997). Effects of chronic beta-adrenergic receptor stimulation in mice. *J Mol Cell*
415 *Cardiol*, 29(10):2735–46.
- 416 Lathers, C. M., Levin, R. M., and Spivey, W. H. (1986). Regional distribution of myocardial β -
417 adrenoceptors in the cat. *European journal of pharmacology*, 130(1-2):111–117.
- 418 Li, R. J., Yang, J., Yang, Y., Ma, N., Jiang, B., Sun, Q. W., and Li, Y. J. (2014). Speckle tracking
419 echocardiography in the diagnosis of early left ventricular systolic dysfunction in type ii diabetic mice.
420 *BMC Cardiovasc Disord*, 14:141.
- 421 Ma, X., Fu, Y., Xiao, H., Song, Y., Chen, R., Shen, J., An, X., Shen, Q., Li, Z., and Zhang, Y. (2015).
422 Cardiac fibrosis alleviated by exercise training is ampk-dependent. *PloS one*, 10(6):e0129971.
- 423 Ma, X., Song, Y., Chen, C., Fu, Y., Shen, Q., Li, Z., and Zhang, Y. (2011). Distinct actions of intermit-
424 tent and sustained β -adrenoceptor stimulation on cardiac remodeling. *Science China Life Sciences*,
425 54(6):493–501.
- 426 Mantravadi, R., Gabris, B., Liu, T., Choi, B.-R., de Groat, W. C., Ng, G. A., and Salama, G. (2007).
427 Autonomic nerve stimulation reverses ventricular repolarization sequence in rabbit hearts. *Circulation*
428 *research*, 100(7):e72–e80.
- 429 Mori, H., Ishikawa, S., Kojima, S., Hayashi, J., Watanabe, Y., Hoffman, J. I., and Okino, H. (1993).
430 Increased responsiveness of left ventricular apical myocardium to adrenergic stimuli. *Cardiovascular*
431 *research*, 27(2):192–198.
- 432 Napp, L. C. and Bauersachs, J. (2020). Takotsubo syndrome: between evidence, myths, and misunder-
433 standings. *Herz*, pages 1–15.
- 434 Paur, H., Wright, P. T., Sikkil, M. B., Tranter, M. H., Mansfield, C., O’gara, P., Stuckey, D. J., Niko-
435 laev, V. O., Diakonov, I., Pannell, L., et al. (2012). High levels of circulating epinephrine trigger
436 apical cardiodepression in a β 2-adrenergic receptor/gi-dependent manner: A new model of takotsubo
437 cardiomyopathy. *Circulation*, 126(6):697–706.
- 438 Pelliccia, F., Kaski, J. C., Crea, F., and Camici, P. G. (2017). Pathophysiology of takotsubo syndrome.
439 *Circulation*, 135(24):2426–2441.
- 440 Peng, Y., Popovic, Z. B., Sopko, N., Drinko, J., Zhang, Z., Thomas, J. D., and Penn, M. S. (2009). Speckle
441 tracking echocardiography in the assessment of mouse models of cardiac dysfunction. *Am J Physiol*
442 *Heart Circ Physiol*, 297(2):H811–20.
- 443 Pfeffer, M. A., Shah, A. M., and Borlaug, B. A. (2019). Heart failure with preserved ejection fraction in
444 perspective. *Circulation research*, 124(11):1598–1617.
- 445 Puhl, S. L., Weeks, K. L., Ranieri, A., and Avkiran, M. (2016). Assessing structural and functional
446 responses of murine hearts to acute and sustained -adrenergic stimulation in vivo. *J Pharmacol Toxicol*
447 *Methods*, 79:60–71.
- 448 Redfors, B., Shao, Y., Wikström, J., Lyon, A. R., Oldfors, A., Gan, L. M., and Omerovic, E. (2014).
449 Contrast echocardiography reveals apparently normal coronary perfusion in a rat model of stress-
450 induced (takotsubo) cardiomyopathy. *Eur Heart J Cardiovasc Imaging*, 15(2):152–7.
- 451 Rona, G. (1959). An infarct-like myocardial lesion and other toxic manifestations produced by isopro-
452 terenol in the rat. *Arch Pathol*, 67:443–455.
- 453 Roussel, E., Drolet, M.-C., Lavigne, A.-M., Arsenault, M., and Couet, J. (2018). Multiple short-
454 chain dehydrogenases/reductases are regulated in pathological cardiac hypertrophy. *FEBS open bio*,
455 8(10):1624–1635.
- 456 Rutledge, C., Cater, G., McMahon, B., Guo, L., Nouraie, S. M., Wu, Y., Villanueva, F., and Kaufman,
457 B. A. (2020). Commercial 4-dimensional echocardiography for murine heart volumetric evaluation
458 after myocardial infarction. *Cardiovascular ultrasound*, 18(1):1–10.
- 459 Sachdev, E., Merz, C. N. B., and Mehta, P. K. (2015). Takotsubo cardiomyopathy. *European Cardiology*
460 *Review*, 10(1):25.
- 461 Sachdeva, J., Dai, W., and Kloner, R. A. (2014). Functional and histological assessment of an experimental
462 model of takotsubo’s cardiomyopathy. *J Am Heart Assoc*, 3(3):e000921.
- 463 Schnelle, M., Catibog, N., Zhang, M., Nabeebaccus, A. A., Anderson, G., Richards, D. A., Sawyer, G.,
464 Zhang, X., Toischer, K., Hasenfuss, G., Monaghan, M. J., and Shah, A. M. (2018). Echocardiographic
465 evaluation of diastolic function in mouse models of heart disease. *J Mol Cell Cardiol*, 114:20–28.
- 466 Shao, Y., Redfors, B., Scharin Täng, M., Möllmann, H., Troidl, C., Szardien, S., Hamm, C., Nef, H.,
467 Borén, J., and Omerovic, E. (2013a). Novel rat model reveals important roles of -adrenoreceptors in

- 468 stress-induced cardiomyopathy. *Int J Cardiol*, 168(3):1943–50.
- 469 Shao, Y., Redfors, B., Ståhlman, M., Täng, M. S., Miljanovic, A., Möllmann, H., Troidl, C., Szardien, S.,
470 Hamm, C., Nef, H., Borén, J., and Omerovic, E. (2013b). A mouse model reveals an important role for
471 catecholamine-induced lipotoxicity in the pathogenesis of stress-induced cardiomyopathy. *Eur J Heart*
472 *Fail*, 15(1):9–22.
- 473 Shao, Y., Redfors, B., Tang, M. S., Assarsson, U., and Omerovic, E. (2013c). Novel simple approach
474 for detection of regional perturbations of cardiac function in mouse models of cardiovascular disease.
475 *Echocardiography*, 30(7):843–9.
- 476 Szymczyk, E., Lipiec, P., Plewka, M., Białas, M., Olszewska, M., Rozwadowska, N., Kamiński, K.,
477 Kurpisz, M., Michalski, B., and Kasprzak, J. D. (2013). Feasibility of strain and strain rate evaluation
478 by two-dimensional speckle tracking in murine model of myocardial infarction: comparison with tissue
479 doppler echocardiography. *J Cardiovasc Med (Hagerstown)*, 14(2):136–43.
- 480 Wallner, M., Duran, J. M., Mohsin, S., Troupes, C. D., Vanhoutte, D., Borghetti, G., Vagnozzi, R. J.,
481 Gross, P., Yu, D., Trapanese, D. M., Kubo, H., Toib, A., Sharp, T. E., r, Harper, S. C., Volkert, M. A.,
482 Starosta, T., Feldsott, E. A., Berretta, R. M., Wang, T., Barbe, M. F., Molquentin, J. D., and Houser, S. R.
483 (2016). Acute catecholamine exposure causes reversible myocyte injury without cardiac regeneration.
484 *Circ Res*, 119(7):865–79.
- 485 Willis, B. C., Salazar-Cantú, A., Silva-Platas, C., Fernández-Sada, E., Villegas, C. A., Rios-Argaiz, E.,
486 González-Serrano, P., Sánchez, L. A., Guerrero-Beltrán, C. E., García, N., Torre-Amione, G., García-
487 Rivas, G. J., and Altamirano, J. (2015). Impaired oxidative metabolism and calcium mishandling
488 underlie cardiac dysfunction in a rat model of post-acute isoproterenol-induced cardiomyopathy. *Am J*
489 *Physiol Heart Circ Physiol*, 308(5):H467–77.
- 490 Wright, P. T., Bhogal, N. K., Diakonov, I., Pannell, L. M. K., Perera, R. K., Bork, N. I., Schobesberger,
491 S., Lucarelli, C., Faggian, G., Alvarez-Laviada, A., Zaccolo, M., Kamp, T. J., Balijepalli, R. C., Lyon,
492 A. R., Harding, S. E., Nikolaev, V. O., and Gorelik, J. (2018). Cardiomyocyte membrane structure
493 and camp compartmentation produce anatomical variation in beta(2)ar-camp responsiveness in murine
494 hearts. *Cell Rep*, 23(2):459–469.
- 495 Zhu, B., Liu, K., Yang, C., Qiao, Y., and Li, Z. (2016). Gender-related differences in β -adrenergic receptor-
496 mediated cardiac remodeling. *Canadian journal of physiology and pharmacology*, 94(12):1349–1355.
- 497 Zhuo, X.-Z., Wu, Y., Ni, Y.-J., Liu, J.-H., Gong, M., Wang, X.-H., Wei, F., Wang, T.-Z., Yuan, Z., Ma,
498 A.-Q., et al. (2013). Isoproterenol instigates cardiomyocyte apoptosis and heart failure via ampk
499 inactivation-mediated endoplasmic reticulum stress. *Apoptosis*, 18(7):800–810.

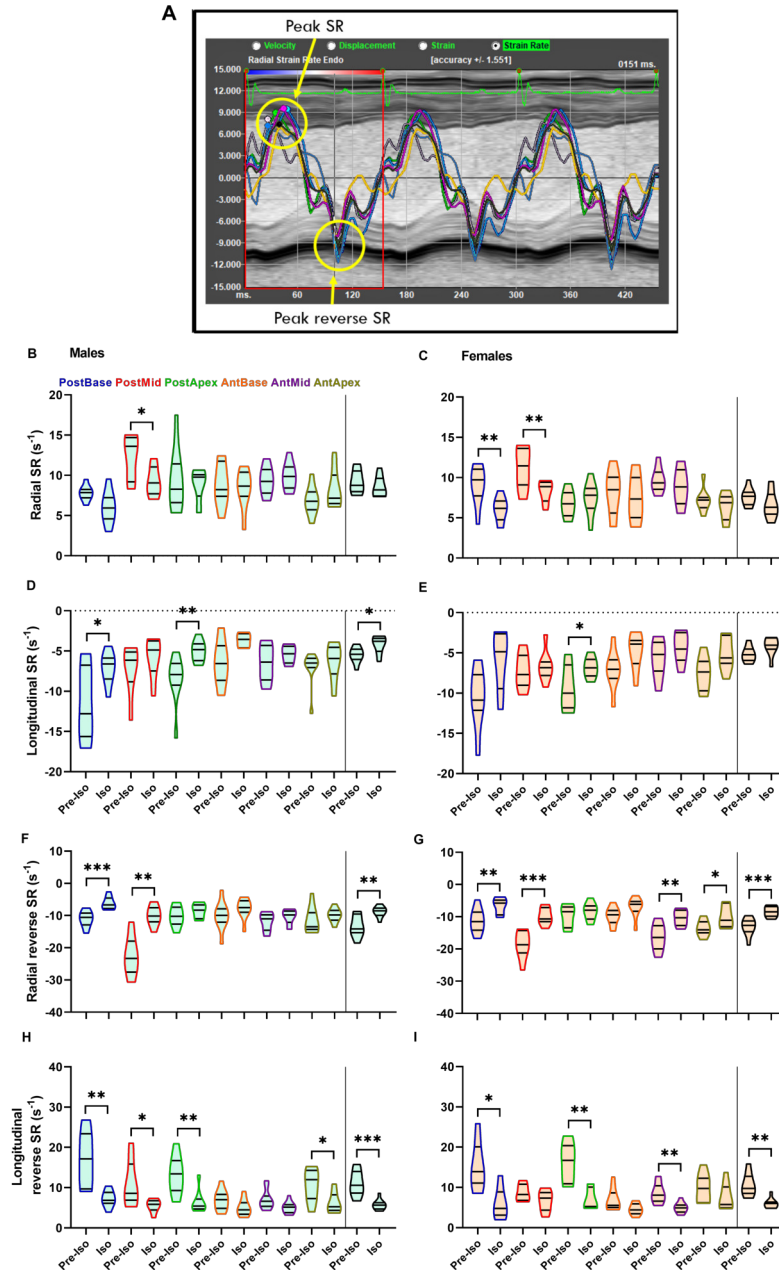


Figure 3. Peak SR and Peak reverse SR (rSR). A. In the background is represented a screen caption of a M-mode loop of three cardiac cycles. In green, the EKG is superposed at the top. Radial strain rate curves are depicted for each SAX segment and as well as an "average" curve in black. Notice that all curves begin at the R wave of the EKG. As evidenced by this representation, the first SR peak (top yellow circle) corresponds to the maximal SR (1/s) whereas the second peak (bottom yellow circle) is inverted and happens during the early stage of LV relaxation as evidenced by the M-mode image underneath. A male mouse after 3 weeks of Iso is represented. B-H. Radial (B-C) and longitudinal (D-E) peak SR as well as rSR (F-H) are illustrated. Characters colors corresponds to those used in the graphs for each of these LV segments. Ant: anterior, Post: posterior, SW: septal wall and FW: free wall. Males are represented on the left panels and females on the right. Results are represented as violin plots (n=8-10). Inner black lines represent quartiles of the data. Significance between groups was calculated with paired Student's T-test. *: p<0.05, **: p<0.01 and ***: p<0.001 between corresponding pre-Iso and Iso groups.

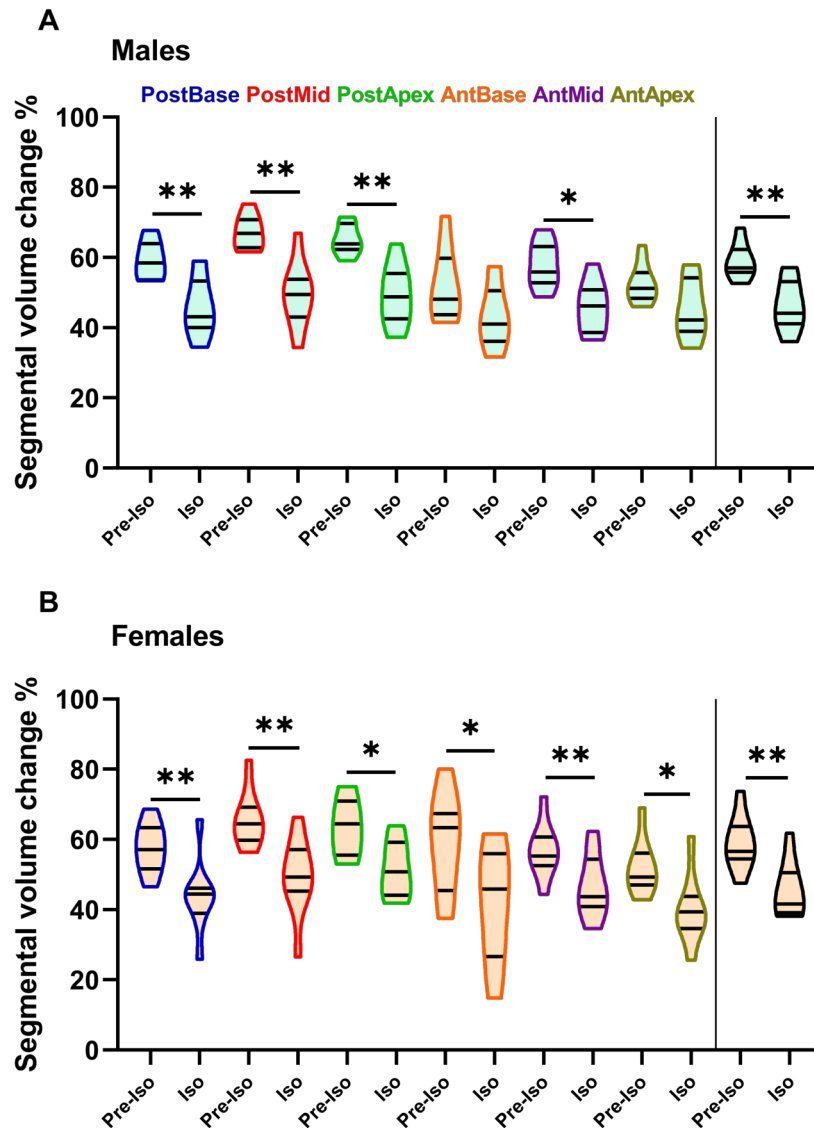


Figure 4. Before-after effects of Iso on segmental volume changes. Relative segmental volume changes are illustrated for males (A) and females (B). Characters colors corresponds to those used in the graphs for each of these LV segments. Ant: anterior, Post: posterior, SW: septal wall and FW: free wall. Males are represented on the left panels and females on the right. Results are represented as violin plots (n=8-10). Inner black lines represent quartiles of the data. Significance between groups was calculated with paired Student's T-test. *: $p < 0.05$ and **: $p < 0.01$ between corresponding pre-Iso and Iso groups.